Spatial and temporal variability of methane emissions and environmental conditions in a hyper-eutrophic fishpond

Petr Znachor[1,2], Jiří Nedoma[1], Vojtech Kolar[1,2], Anna Matoušů[1]

[1]Biology Centre of Czech Academy of Sciences, v.v.i., Institute of Hydrobiology, Na Sádkách 7, České Budějovice, 37005, Czech Republic

[2]Faculty of Science, University of South Bohemia, Branišovská 1760, České Budějovice, 37005, Czech Republic

Correspondence to: Anna Matoušů (anna.matousu@gmail.com)

Abstract. Estimations of methane (CH_4) emissions are often based on point measurements using either flux chambers or a transfer coefficient method which may lead to strong underestimation of the total CH_4 fluxes. In order to demonstrate more precise measurements of the CH_4 fluxes from an aquaculture pond, using higher resolution sampling approach we examined the spatiotemporal variability of CH_4 concentration in the water, related fluxes (diffusive and ebullitive) and relevant environmental conditions (temperature, oxygen, chlorophyll-a) during three diurnal campaigns in a hyper-eutrophic fishpond. Our data show remarkable variance spanning several orders of magnitude while diffusive fluxes accounted for only a minor fraction of total CH_4 fluxes (4.1–18.5 %). Linear mixed-effects models identified water depth as the only significant predictor of CH_4 fluxes. Our findings necessitate complex sampling strategies involving temporal and spatial variability for reliable estimates of the role of fishponds in a global methane budget.

Keywords: aquaculture, emissions, fishpond, freshwater, heterogeneity, methane

1 Introduction

Freshwater aquaculture ponds (fishponds) represent man-made counterparts to natural shallow lakes (Scheffer, 2004) which are mainly used for fish production (mostly of common carp, *Cyprinus carpio* L.) and water retention in the landscape. Fishponds serve also as secondary biotope for various organisms (Kolar et al., 2021), supporting noteworthy animal and plant diversity (Pokorný and Hauser, 2002). However, most fishponds suffer from high fish stock densities, excessive carbon and nutrient loading from supplemental fish feeding, sewage pollution, and fertiliser runoffs from agricultural catchments or nutrient mobilisation from the anoxic sediment layers (Pechar, 2000). As a result, the trophic structure of plankton communities has shifted towards a reduction of large zooplankton and massive development of phytoplankton, especially cyanobacterial blooms (Potužák et al., 2007), limiting light penetration in the water column. Rapid changes in the intensity of biological processes such as photosynthesis and respiration often result in pronounced daily or seasonal fluctuations in dissolved oxygen (Baxa et al., 2021), signalling decreasing ecosystem stability. The extent of anoxia, accumulation of organic biomass, and rapid heating of the shallow water during summer result in enhanced production of greenhouse gases (Grasset et al., 2018, Zhang et al., 2021; Bartosiewicz et al., 2021).

Most concerning are CH_4 emissions as freshwater aquaculture systems release more than 6 Tg CH_4 yr^{-1} (Yuan et al., 2019). Methane can be emitted via several pathways: simple molecular diffusion, ebullition (in the form of bubbles released from oversaturated sediments), plant-mediated flux (Bastviken et al., 2004), but also through so far neglected pathways including aeration, emissions from dry/drying sediments, or dredged organic material (Kosten et al., 2020). Among all, ebullition is considered the dominant pathway (van Bergen et al., 2019; Kosten et al., 2020), which can contribute 50–96 % (Casper et al., 2000; Xiao et al., 2017; van Bergen et al., 2019; Yang et al., 2020; Zhao et al., 2021) to the total CH_4 flux. Along with the second important pathway – molecular diffusion, both exhibit high spatiotemporal variability due to various physical and biological factors acting on very short time scales, for instance, temperature (van Bergen et al., 2019), nutrient loading (Zhang et al., 2021), CH_4 production rates (Zhou et al., 2019), CH_4 oxidation rates (Sanseverino et al., 2012), dissolved oxygen concentration (Xiao et al., 2017), management regime (Yang et al., 2019), or the quality of organic matter in the sediment (Schmiedeskamp et al., 2021). Recently, the ~~direct~~ potential involvement of phytoplankton in CH_4 production and emissions has been ~~emphasised~~ suggested (Yan et al., 2019; Bižić et al., 2020; Bartosiewicz et al., 2021). The complex interactions between physical and biological factors lead to a dynamic and ever-changing environment, characterised by high spatial and temporal variability of methane fluxes in ponds.

Although fishponds are recognised as powerful model systems for studies in ecology and evolutionary or conservation biology (De Meester et al., 2005; Céréghino et al., 2008), the extent of environmental heterogeneity in fishponds and shallow inland small waterbodies remains poorly understood (Ortiz and Wilkinson, 2021), largely because the driving factors are either system-specific or highly variable on short time scales (Laas et al., 2012). Most of current information on lentic ecosystem structure and function comes from single-site sampling, in which measurements are taken over time at the deepest point in the lake, which does not sufficiently account for within-lake spatial variation (Stanley et al., 2019). The motivation for our study was the growing concern about the role of fishponds as important sources of CH_4 fluxes to the atmosphere (Wik et al., 2016). Unfortunately, the majority of global CH_4 flux estimates rely on upscaling methods (DelSontro et al., 2018a) based on a limited number of measurements that do not account for diurnal and seasonal variability or ecosystem spatial heterogeneity. Yang et al. (2019) indicates that a larger number of spatial replicates over a number of months is mandatory to improve the accuracy of whole-pond CH_4 flux estimates. The published research from other aquaculture studies have been performed mainly in tropical and subtropical zones in fish or crab aquacultures (e.g., Hu et al., 2016; Ma et al., 2018; Yang et al., 2019, 2020; Yuan et al., 2019, 2021). To better understand the spatial dynamics of CH_4 fluxes and environmental heterogeneity in temperate freshwater shallow lake, we conducted a spatial sampling of the hyper-eutrophic Dehtář fishpond (Czech Republic, Europe). Since the seasonal CH_4 production is strongly affected by temperature, we focused on warm summer months where the total CH_4 fluxes were expected to be the highest (Jansen et al., 2019). The objectives of our study were (i) to determine the spatial heterogeneity of CH_4 diffusive and total fluxes and fundamental limnological variables (oxygen, temperature, chlorophyll-a) and their change daily and monthly in the hyper-eutrophic pond, and (ii) to identify the factors that influence CH_4 fluxes to improve our understanding of the importance of spatiotemporal variability for global estimates of CH_4 efflux to the atmosphere.

2 Material and Methods

2.1 Study site description

The Dehtář fishpond (49°00'24.4"N 14°17'39.3"E49° N, 14° E) is a shallow man-made lake (average and maximum depth: 2.4 and 6 m) constructed in 1479 and used for polycultural, semi-intensive production of common carp (Potužák et al., 2016). It is used for polycultural, semi-intensive production of common carp, which account for 90–95 % of the fish biomass (Rutegwa et al., 2019). The pond is stocked with two-year old carp harvested at

the end of a two-year production cycle. To increase fish production, the original management, based mainly on natural processes, has been intensified, and today manuring and supplementary feeding in the form of grain or fish pellets, are common practices (Pechar, 2000). It The pond lies in a flat agricultural landscape at 406.4 m above sea level in the upper Vltava River basin in South Bohemia (Czech Republic) which is characteristic with its network of fishponds (Fig. 1b). Due to the orography of the landscape, the Dehtář fishpond, surrounded by narrow belts of littoral vegetation and adjacent to grassland and arable land, is exposed to wind, mainly from the northwest (for aerial photograph, see Suppl. Fig 1). The catchment area is 91.4 km^2. The main inflow is the Dehtářský stream in the south, while several smaller tributaries flow in from the west (Fig. 1c). The fishpond has a dam 234 m long and 10 m high, with two outlets and a safety spillway. Covering 2.28 km^2, the Dehtář fishpond is among the ten largest fishponds in the Czech Republic, holding a volume of 4.71×10^3 m^3 and having a water residence time of 146 - 445 days (Potužák et al., 2016).
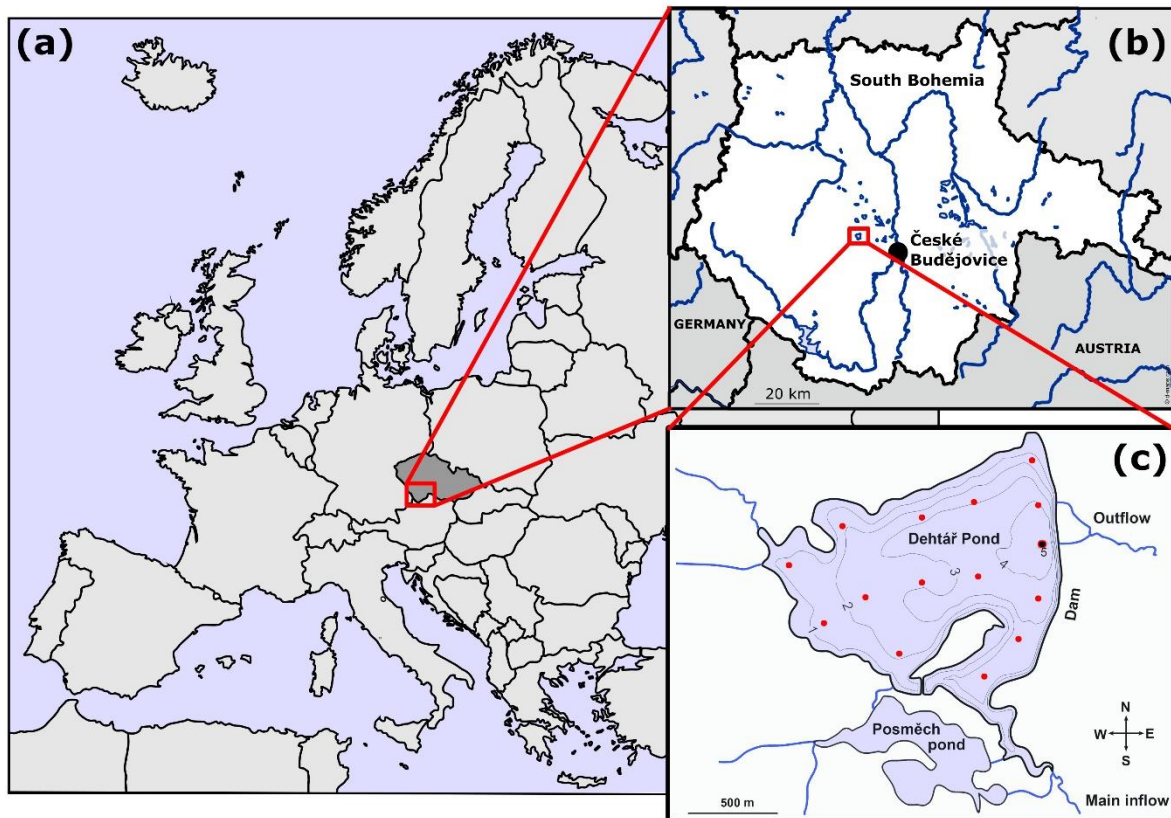
Figure 1. Location (a, b; copyright www.d-maps.com; https://d-maps.com/carte.php?num_car=2232&lang=en and https://d-maps.com/carte.php?num_car=265046&lang=en; modified) and bathymetric map (c; credit Jiří Jarošík) of the sampled Dehtář fishpond: blue lines indicate hydrological connections; red dots representing the sampling points. Highlighted sampling point at the dam depicts the deepest site where vertical profiles were measured. Numbers indicate isobath depth.

2.2 Sampling design and measurement

To measure spatial heterogeneity and temporal changes in limnological parameters and methane fluxes, we conducted three 36-hour surveys in summer 2019 (July 2–3, August 13–14, September 19–20). In the morning (between 5–6 a.m.), we first measured surface values and vertical profiles of temperature, oxygen, and chlorophyll-*a* concentration at the deepest point (see below for details). We subsequently installed 15 floating polyethylene chambers (as shown in Fig. 1c), serving as fixed sampling sites and at the same time for accumulation of CH_4 fluxes (see further), starting in the western part of the fishpond. During installation (and further during each sampling), temperature, pH, and oxygen concentration were measured at 0.3 m depth using the WTW 330i pH meter and Oximeter (WTW, Weilheim, Germany). Vertical chlorophyll-*a* profiles were measured at each sampling site using a submersible fluorescence probe (FluoroProbe, bbe Moldaenke, Kiel, Germany). From each site, the average chlorophyll-*a* concentration in the surface layer (0–1 m depth) was used to assess the phytoplankton spatial heterogeneity.

To minimise the chance that the differences observed among sites were due to time of day, we conducted repeated measurements at the deepest point at the end of each sampling. This was relevant mainly to the initial measurement, when the installation of all floating chambers took a total of 3 hours and 50 minutes. All other measurements, i.e., the interval between the first and last sampling point, required approximately two hours each. If there was a change, all values were corrected for the sampling time by linear interpolation:

$$P_{corr} = P_t + (P_{end} - P_0) \times \frac{(t - t_0)}{(t_{end} - t_0)} \tag{1}$$

where P_{corr} is the corrected value of a parameter, P_t is its value measured at the time t, P_0 and P_{end} are parameter values measured at the deepest point at the start (time t_0) and at the end (t_{end}) of the sampling. In the evening and morning of the second day (roughly at 12 h intervals), we performed additional measurements of spatial heterogeneity, allowing us to assess diurnal and nocturnal changes. In addition, samples for measuring CH_4 concentration in the surface water were collected at each site and analysed as described below. To assess diurnal variations in thermal structure and oxygen concentration in the water column, we made vertical profile measurements at the deepest point (Fig. 1c) at 3–6 h intervals using the YSI EXO 2 multiparametric probe (YSI Inc., Yellow Springs, USA).

2.3 Methane measurements

Water samples for determining CH_4 concentration in the surface water were collected at all 15 sampling sites in triplicates into 20 ml glass bottles. The bottles were capped bubble-free under water with black butyl rubber stoppers (Ochs, Germany) and sealed with aluminium crimps. Immediately after sampling, the water samples were

127   preserved by injecting 100 μL of concentrated sulfuric acid to stop the microbial activity (Bussmann et al., 2015).

128   The samples were processed within one week in the laboratory using a headspace technique according to

129   McAuliffe (1971). Methane concentration in the headspace was measured using an HP 5890 Series II gas

130   chromatograph (Agilent Technologies, USA) and calculated with the solubility coefficient given by Yamamoto et

131   al. (1976).

132   Methane diffusive fluxes (F) were then calculated for each sampling site indirectly using the 2-layer model with

133   the equation:

134     $F = k(C_{sur} - C_{eq})$ (2)

135   where C_{sur} is the CH_4 concentration in surface water in μmol L^{-1}, C_{eq} is the CH_4 concentration in surface water in

136   equilibrium with the atmosphere in μmol L^{-1}, and k is the CH_4 exchange constant (cm h^{-1}). The atmospheric partial

137   pressure of CH_4 was set to 1.8 ppm. To compute k values, we first derived k_{600} estimates using a wind speed-based

138   relationship according to Crusius and Wanninkhof (2003):

139     $k_{600} = 1.68 + (0.228 \times U_{10}^{2.3})$ (3)

140   where U_{10} represents the wind speed at 10 m height (in m s^{-1}; obtained from the nearby gauging station)

141   approximated by $U_{10} = 1.22U$, where U is the wind speed at 1.5 m height. We then converted k_{600} to k using the

142   eq. 4 according to Crusius and Wanninkhof (2003):

143     $k = k_{600} \left(\frac{Sc}{600}\right)^n$ (4)

144   where k_{600} is the gas transfer velocity for a Schmidt number (Sc) of 600; n is a wind speed-dependent conversion

145   factor, for which we used $-2/3$ for $U_{10} < 3.7$ m s^{-1} (Jähne et al., 1987). The Schmidt number for CH_4 was calculated

146   according to Wanninkhof (2014):

147     $Sc = 1909.4 - 120.78t + 4.1555t^2 - 0.080578t^3 + 0.000658t^4$ (5)

148   where t (°C) is the water temperature at the time of CH_4 extraction. The parameter C_{eq} in Eq. (1) was determined

149   from the equation:

150     $C_{eq} = \beta \times pCH_4$ (6)

151   where β is the solubility coefficient of CH_4 as a function of temperature according to Wiesenburg and Guinasso

152   (1979), and pCH4 is the partial pressure of CH_4 in the atmosphere.

153   To estimate total CH_4 fluxes from the water column to the atmosphere (i.e., diffusive and ebullitive fluxes), we

154   measured CH_4 accumulation in open-bottom floating polyethylene chambers (volume 3.1 L; area 0.024 m^2). Each

155   gas chamber was anchored at individual 15 fixed sampling sites, but allowed to float freely on the water surface.

156   Gas was accumulating for approximately 12 h (each incubation had a start and end point) during particular

157 sampling period, i.e., during the day and night periods. Afterwards, 30 ml of gas was carefully taken from each

158 chamber, after mixing the headspace in the chamber, and stored in evacuated Exetainers® (Labco Limited, UK).

159 Chambers were ventilated after each sampling period to reset the incubation conditions. Methane fluxes were

160 calculated as the difference between initial background and final concentration in the chamber headspace and

161 expressed on the 1 m^2 area of the surface level per day according to Bastviken et al. (2004).

162 **2.4 Background limnological parameters**

163 During each campaign, water samples for analysis of nutrient concentration and phytoplankton composition were

164 collected from the surface at the deepest point using a Friedinger sampler. Water transparency was measured using

165 a Secchi disk. Total phosphorus (TP) and soluble reactive phosphorus (SRP) were analysed spectrophotometrically

166 according to Kopáček and Hejzlar (1993) and Murphy and Riley (1962), respectively. Concentrations of NH_4^+ and

167 NO_3^- were determined according to the procedure of Kopáček and Procházková (1993) and Procházková (1959),

168 respectively. Phytoplankton samples were preserved with Lugol's solution and examined for species composition

169 with an inverted microscope (Olympus IMT-2). Weather data were obtained from the gauging station at the

170 fishpond dam.

171 **2.5 Statistical analyses**

172 Two-tailed paired Student's t-tests and Two-way ANOVA with post-hoc Tukey's multiple comparison test (Prism

173 9.3, GraphPad Software Inc., La Jolla, USA) tested for differences between diffusive and total CH_4 fluxes between

174 day and night and among three sampling campaigns, respectively. The percentage of data variability explained by

175 different factors (daytime, month and site) was calculated with the Two-way RM ANOVA. Contour graphs

176 illustrating changes in spatial heterogeneity of measured parameters were constructed in Surfer 10 (Golden

177 Software, Inc., Colorado, USA) using the kriging contouring method. Spatial heterogeneity was quantified for

178 each sampling by calculating the spatial variance (i.e., coefficient of variation of values measured at 15 sampling

179 sites; see, e.g. Fig 2):

180 $$CV\% = 100 \times \frac{SD}{mean} \tag{7}$$

181 Higher spatial variance indicates increasing ecosystem patchiness. Linear mixed-effects models were used to

182 analyse the effects of O_2, pH, temperature, and water depth on the CH_4 diffusive fluxes with the random effect of

183 time of day nested within the effect of sampling date. The most parsimonious model was obtained by a manual

184 backward selection, where we sequentially removed all insignificant predictors (p > 0.05) using likelihood ratio

tests implemented in the drop1 function (Zuur et al., 2009). We also compared the slopes of the month-specific regression lines produced by the model using analysis of covariance (Zar, 1984). Linear mixed-effects models were implemented in the lme4 package version 1.1-21 (Bates et al., 2015), and Kenward-Roger F-tests were computed using the ANOVA Type II function from the pbkrtest package version 0.4-7 (Halekoh and Hojsgaard, 2014). The prediction of the resulting final model was visualised in the package ggeffects version 0.14.1 (Lüdecke, 2018). Package performance version 0.4.4 (Lüdecke et al., 2020) was used to calculate Nakagawa's R^2 of the linear model. The statistical analyses were performed using R software (v. 3.5.2, R Core Team, 2018).

3 Results

3.1 Weather and background fishpond characteristics

Weather parameters varied among sampling campaigns. In July, clear skies prevailed with the daily air temperature above 30 °C (Table 1). During the August and September measurements, it was very cloudy, and daily air temperatures decreased to 22 and 18 °C, respectively. The water level was stable during the whole studied period with a monthly fluctuation of ~ 10 cm. Water transparency was low (15–40 cm), with an increasing trend towards the end of summer (Table 1). Concentrations of total phosphorus and soluble reactive phosphorus were high (Table 1), consistent with a hyper-eutrophic state of the fishpond. In contrast, nitrogen concentrations were rather low, with ammonium nitrogen being the predominant form of inorganic N in the water (Table 1).

Table 1: Basic characteristics of the Dehtář fishpond during the studied period, measured at the surface at the deepest point.

	July	August	September
Weather	Clear sky, windy	Partly cloudy, no wind	Partly cloudy, no wind
Air temperature (°C)	25–32	20–22	11–18
Water temperature (°C)	24—29	22—23	16—17
Maximum wind speed (m s^{-1})	3.2	0.8	0.9
PHAR (mol m^{-2} day^{-1})	9.5	3.4	5.0
Secchi depth (cm)	15	30	40
TP (µg L^{-1})	568	527	406
SRP (µg L^{-1})	100	200	107
N-NH$_4^+$ (µg L^{-1})	23	783	560
N-NO$_3^-$ (µg L^{-1})	14	23	46

Chl-*a* (µg L⁻¹)	456	156	185
Phytoplankton composition	Cyanobacteria	Cyanobacteria, green algae, cryptophytes	Cryptophytes, green algae

Chlorophyll-*a* concentrations were highest in July due to the dense cyanobacterial bloom accumulated at the surface (Table 1). The phytoplankton consisted of only three cyanobacterial taxa: *Dolichospermum flos-aquae, Planktothrix agardhii,* and *Raphidiopsis mediteranea*. In August, phytoplankton was more diverse but also dominated by cyanobacteria: *P. agardhii, Aphanizomenon issatschenkoi,* and *D. flos-aquae*. In September, cyanobacteria were absent and instead, cryptophytes (*Cryptomonas reflexa*), green algae (*Pediastrum, Coelastrum* and *Desmodesmus*) and dinoflagellates (*Ceratium hirundinella*) prevailed.

3.2 Methane concentration and fluxes

The CH_4 concentration in surface water was highly supersaturated over the whole studied period. The obtained values varied from 0.003 up to 3.75 µmol L⁻¹ (Fig. 2), which corresponded to saturation levels of 108–12 834%. It is obvious, that the obtained data show remarkable variance: the mean ($\pm$ SD) values were 0.22 $\pm$ 0.18 for July, 0.34 $\pm$ 0.45 for August, and 1.61 $\pm$ 0.61 µmol L⁻¹ for September (Suppl. Fig. 11).
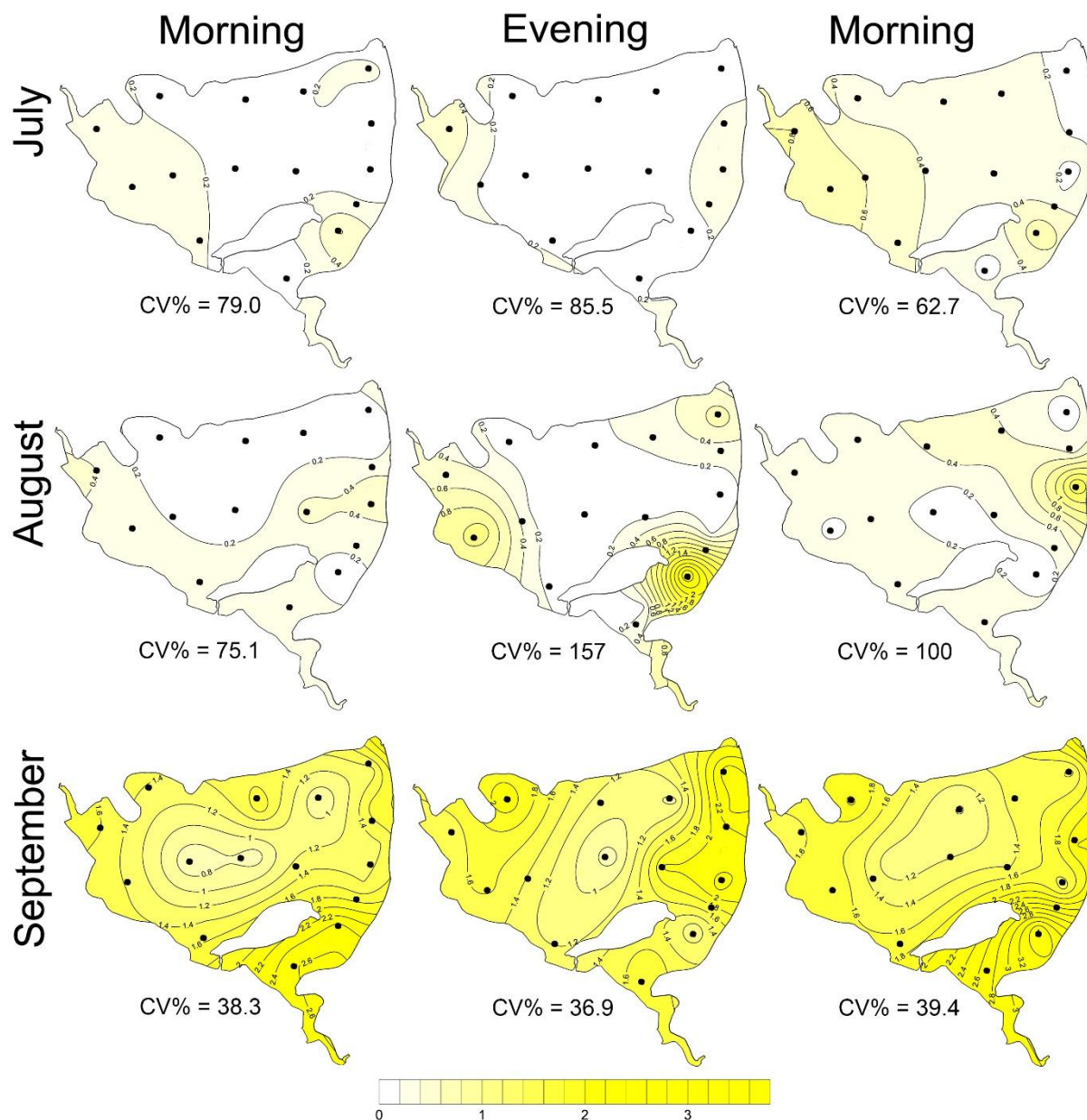
Figure 2: Surface methane concentrations (µmol L^{-1}). Contour graphs illustrating both seasonal and daily changes in spatial heterogeneity (indicated by the coefficient of variation, CV%) in the fishpond. Black dots representing the sampling sites.

Diffusive fluxes (i.e., calculated from CH$_4$ concentration, see Eq. 2) showed the lowest values in July and August (average 0.12 and 0.16 mmol m^{-2} d^{-1}, respectively) and pronouncedly peaked in September (average 0.78 mmol m^{-2} d^{-1}, Fig. 3a). By contrast, in July and August, the average total CH$_4$ fluxes (obtained with floating chambers) showed the highest values (average 31.8 mmol m^{-2} d^{-1}; ranging from 0.08 to 152 mmol m^{-2} d^{-1}) while in September, total CH$_4$ fluxes were three times lower than before (average 11.8 mmol m^{-2} d^{-1}, range 0.3 to 43.5 mmol m^{-2} d^{-1}, Fig 3b). As a result, diffusive fluxes accounted for only a minor fraction of total CH$_4$ fluxes to the atmosphere (on average, 9.2 % in July, 4.1 % in August, 18.5 % in September, Fig. 3c).

226
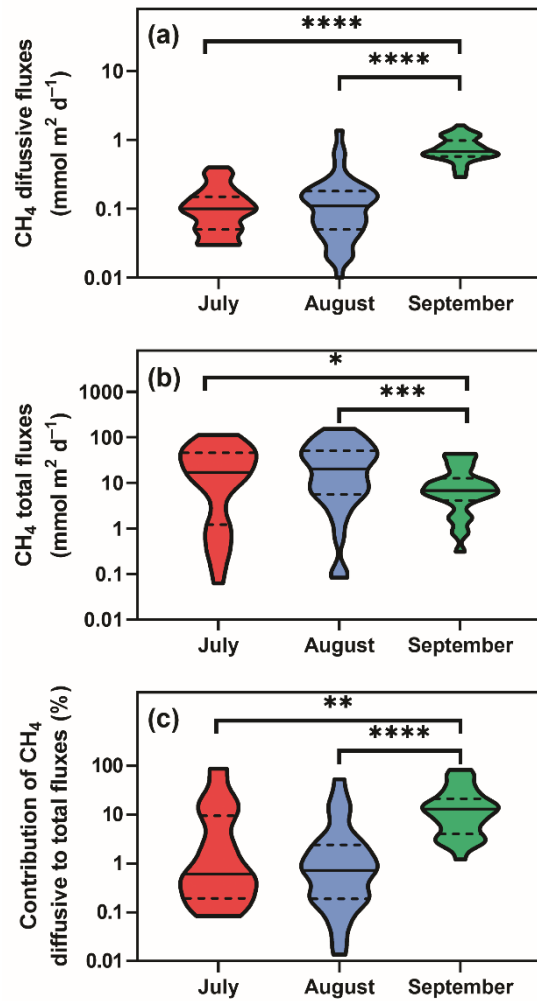
Figure 3: Violin plots of CH_4 diffusive (a) and total fluxes (b) during the studied period. Panel (c) depicts differences in the percentage contribution of diffusive to total fluxes. Solid lines are medians, while dashed lines denote quartiles. Asterisks indicate significant differences (* $p<0.05$, ** $p<0.01$, *** $p<0.001$, **** $p<0.0001$) between sampling dates determined by two-way ANOVA with Tukey's multiple comparison test. Note that a log scale is used here for clarity.

The total CH_4 fluxes show spatial variability within the fishpond that range four orders of magnitude (Fig. 3, 4; Suppl. Fig. 11; Suppl. Table 1). The observed spatial pattern showed high temporal variability on both daily and monthly scales (Fig. 2, 4, Suppl. Table 1). Most of the variability in CH_4 diffusive fluxes was explained by sampling date (62.4 %), while for the total CH_4 fluxes, spatial heterogeneity accounted for 87.2 % of data variability (Table 2). Using linear mixed-effects models, we identified water depth as the only significant predictor of total CH_4 fluxes (Df = 1, $p < 0.0001$, marginal Nakagawa's $R^2 = 0.348$; Fig. 5).

241 **Table 2**: The percentage of data variability explained by different factors (daytime, month = sampling date, and site)

242 calculated with the Two-way RM ANOVA. Statistically significant values (p < 0.01) are bold.

	% of variability				Significance		
	Daytime	**Month**	**Site**	**Unexplained**	**Daytime**	**Month**	**Site**
CH_4 diffusive flux	2.3	**62.4**	13.2	22.1	0.0123	<0.0001	*n.s.*
CH_4 total flux	0.19	2.4	**87.2**	10.2	*n.s.*	*n.s.*	<0.0001
pH	**4.4**	**64.9**	11.1	19.6	0.0001	<0.0001	*n.s.*
Water temperature	**3.3**	**92.3**	**2.5**	1.9	<0.0001	<0.0001	<0.0001
O_2	**21.7**	**48.1**	13.8	16.4	<0.0001	<0.0001	0.0135
Chl-*a*	0.019	**74.9**	**16.7**	8.4	*n.s.*	<0.0001	<0.0001

243 Interestingly, slopes of the linear regressions differed significantly among individual sampling campaigns (Fig. 5),

244 indicating an additional season-related factor that affects CH_4 fluxes in the fishpond. Calculated CH_4 diffusive

245 fluxes were not correlated with total fluxes. Linear mixed-effects models did not identify any significant predictor

246 of the fluxes, indicating that factors and processes out of the study's scope are involved. We found no significant

247 difference in either diffusive or total CH_4 fluxes between day and night.

248
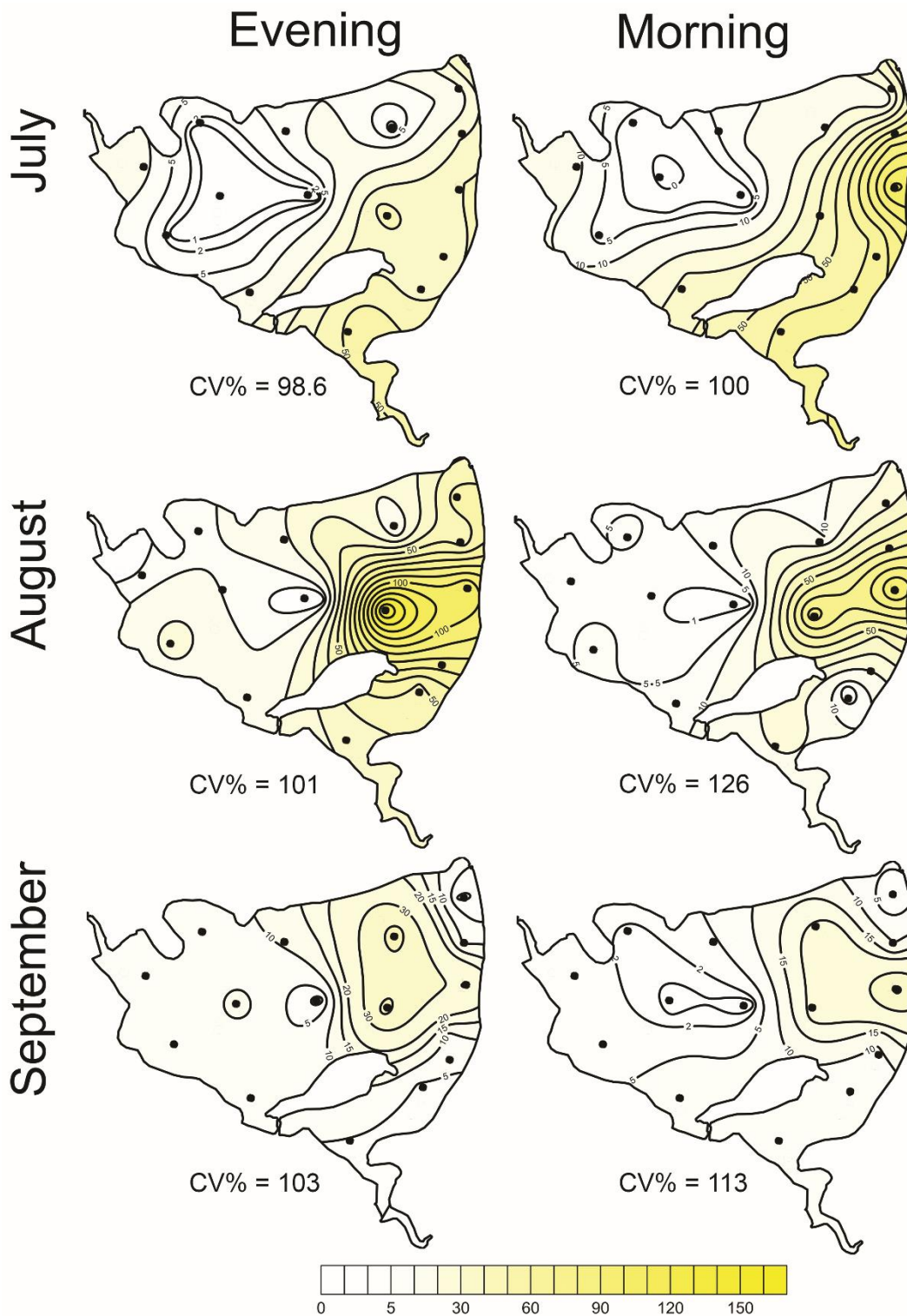
Figure 4: Contour graphs of methane total fluxes in the Dehtář fishpond. Isopleths connect sites with the same value of methane fluxes (mmol m^{-2} day^{-1}). CV% is a measure of spatial heterogeneity. Black dots representing the sampling sites.

251
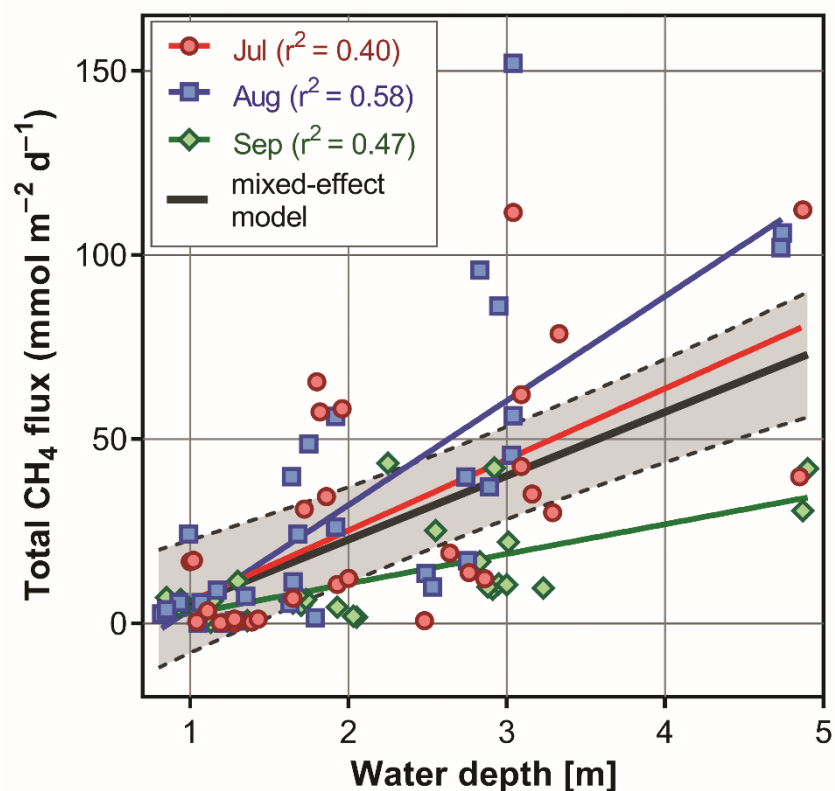
Figure 5: The most parsimonious linear mixed-effect model of methane total fluxes showing the water depth as the only significant predictor. Symbols are the measured values, the solid black line is the prediction, and dashed lines are 95th confidence intervals. Colours indicate month specific relation between total methane fluxes and water depth. Differences in slopes were tested using the F-test. In September, the slope of the regression line was significantly different from that in July and August.

3.3 Diurnal changes in vertical profiles of oxygen and temperature

Several contrasting patterns of vertical temperature and oxygen profiles occurred during summer 2019. Diurnal changes were most pronounced in July (Fig. 6). Surface temperatures varied from 25 °C in the morning to nearly 30 °C in the afternoon. Thermal stratification of the water column was weak in the morning but became strongest at 14:30 with a thermocline at 0.5 m depth (Fig. 6). Later in the afternoon, the water column began to be mixed by wind. The morning vertical oxygen profile was characterised by a surface value of 4.3 mg L^{-1}, corresponding to 51 % saturation and anoxia below 3 m.
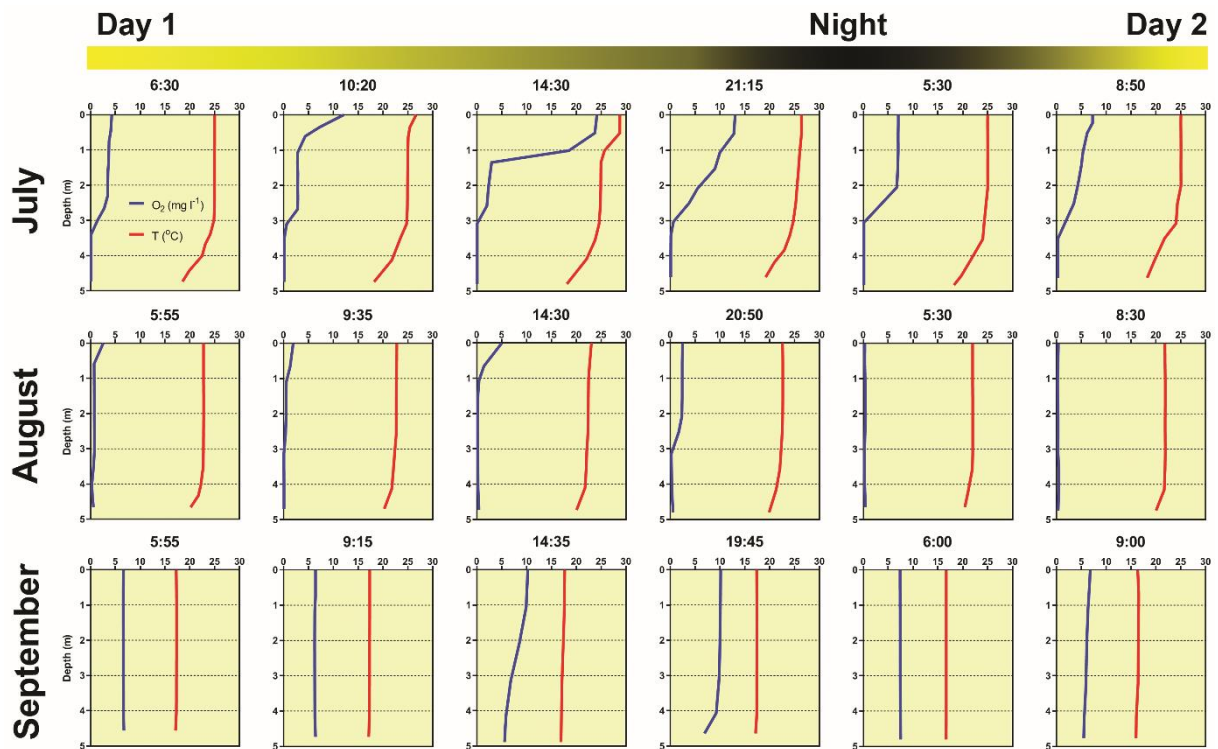
Figure 6: Diurnal changes in vertical profiles of temperature and oxygen concentration measured at the deepest point of the fishpond. Numbers above each graph indicate the time of measurement.

Due to the high photosynthetic activity of cyanobacteria, the surface oxygen concentration increased to 24 mg L^{-1} (320 % saturation, Fig. 6), and a steep oxycline was established at a depth of 0.5–1.5 m with no effect on the anoxic conditions at the deeper layers. Wind action eroded both the oxy- and thermoclines in the evening, and by the next morning, the vertical profiles were similar to those at the beginning.

In August, the water column was almost entirely mixed and low in oxygen in the morning, with only 2.6 mg L^{-1} (30 % saturation) of oxygen at the surface. Due to cloudy weather, the daily photosynthetic activity of phytoplankton resulted in only a slight increase in oxygen concentration at 0–1.5 m depth (4 mg L^{-1}, 47 % saturation). By the morning of the next day, the entire water column turned very close to anoxic (0.4 mg L^{-1}, 4 % saturation; Fig. 6), which in turn affected the spatial distribution of zooplankton, as evidenced by the formation of dense zooplankton clouds accumulated in the thin layer just at the surface (see Suppl. Fig. 3). In September, the water column was completely mixed, and we observed only weak daily changes in thermal and oxygen vertical structures (Fig. 6).

3.4 Effect of wind on spatial heterogeneity of temperature, oxygen and chlorophyll-*a*

During the summer, all measured parameters showed remarkable within-lake spatial heterogeneity (Suppl. Fig. 5––8). In July, meteorological conditions allowed for demonstrating the effect of wind on fishpond spatial

heterogeneity. In the morning, there were no substantial differences in the surface temperature and oxygen concentrations (Fig. 7ab). Phytoplankton biomass was accumulated mostly in the shallow western part, with the maximum in the centre (Fig. 7c). At 14:00, a light breeze started to blow from the northwest, achieving a maximum of 3.2 m s^{-1} (Suppl. Fig. 9). This episode lasted till the evening measurement, and the wind ceased by 21:00. The wind was strong enough to change spatial distribution substantially (Fig. 7d–f, Suppl. Fig. 4). In the evening, the surface water temperature on the windward (south) side of the fishpond was ~ 4 °C higher than in the north (Fig. 7d). The wind also induced order of magnitude differences in oxygen concentration along the north-south axis of the fishpond (3 mg L^{-1} of O$_2$ at the north, 24 mg L^{-1} of O$_2$ at the south; Fig. 7e) and affected phytoplankton distribution in the fishpond, resulting in remarkable bloom accumulation in the south (Fig. 7f, Suppl. Fig. 8). During the calm night after the disturbance, the north-south gradient substantially weakened. In August and September, the thermal heterogeneity of the pond was rather low, but the spatial distribution of oxygen and chlorophyll-*a* remained highly variable (Suppl. Fig. 5–8, Suppl. Table 1).
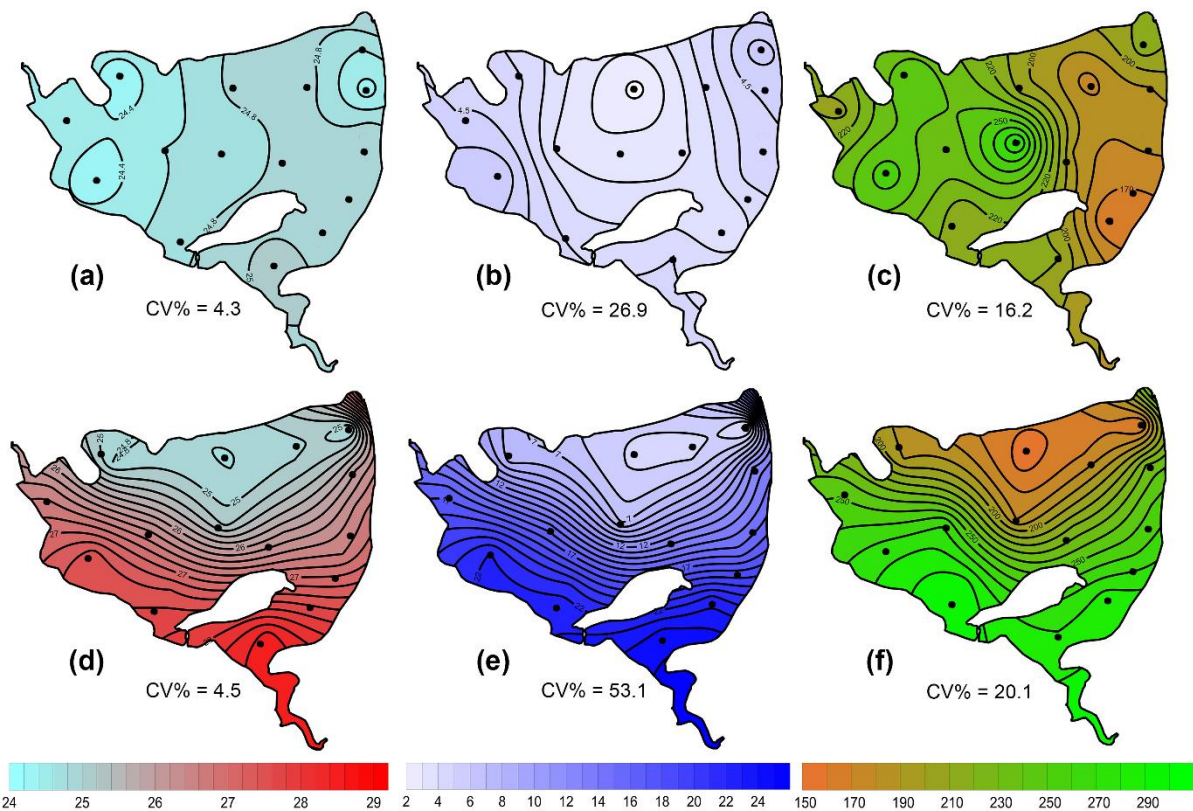
Figure 7: Contour graphs of surface temperature (a, d; °C), oxygen concentration (b, e; mg L^{-1}) and chlorophyll-a concentration (c, f; μg L^{-1}) measured on July 2 at different times of day: a, b and c are the morning measurements; d, e and f are evening measurements following a wind disturbance. Coefficient of variation (CV %) is a measure of spatial heterogeneity of measured parameters. Black dots representing the sampling sites.

4 Discussion

4.1 Methane fluxes

Assessing spatial heterogeneity of the CH_4 fluxes within a fishpond is critical for a reliable estimate of its contribution to the global CH_4 budget. In our study, the variability in total CH_4 fluxes spanned several orders of magnitude (ranging from 0.06 up to 1 121.3 mmol m^{-2} d^{-1}), which is in agreement with similar studies (Casper et al., 2000; DelSontro et al., 2016; Natchimutu et al., 2016). However, most system-specific CH_4 flux estimates rely on upscaling from a limited number of sites (Bastviken et al., 2004; Rasilo et al., 2015; Wik et al., 2016) because obtaining spatial variability in CH_4 emission is methodologically challenging. In general, spatial heterogeneity may reflect differences in water sources, physical mixing, local transformations and biogeochemical processes and rates among lake habitats (Loken et al., 2019). In deep lakes, littoral areas can contribute disproportionately to total lake CH_4 fluxes (Hofmann et al., 2010; Hofmann 2013, Natchimuthu et al., 2016; Schilder et al., 2013) and are often missed by traditional sampling approaches (Wik et al., 2016). According to Wik et al. (2016), low temporal and spatial resolutions are unlikely to cause overestimates. On the other hand, DelSontro et al. (2018b) suggested that horizontal transport of CH_4 produced in littoral zones and the interaction between physical and biological processes (e.g. air-water gas exchange, water column mixing, the interplay between CH_4 production and microbial oxidation) may result in an underestimation of whole-lake CH_4 fluxes based on centre samples. Similarly, Natchimuthu et al. (2016) found that up to 78 % underestimation would occur if samples obtained only from the lake centre are used to extrapolate the total CH_4 flux. However, extrapolating our data from the deepest point of the Dehtář fishpond would lead to an overestimation of the CH_4 fluxes by a factor of 2.9 (Suppl. Fig. 12). The bias introduced by the deepest point measurement appears to be highly variable among systems with different morphology, geographical location, mixing regimes or trophic states. For instance, analysis of 22 European lakes during late summer has shown that spatially resolved CH_4 diffusive fluxes were highly variable for individual lakes, yielding 55–300 % differences in the whole-lake estimates (Schilder et al., 2013). Schmiedeskamp et al. (2021) observed an increase in CH_4 fluxes from the shore towards the centre in response to increasing sediment C-content in two shallow German lakes. In line with these findings, our results provide further evidence that spatially resolved data are needed to validate the uncertainties that come from using single-point samples to represent whole-lake processes in hyper-eutrophic systems. As stated by Loken et al. (2019), rather than assuming spatial homogeneity, scaling-up exercises of global carbon budgets should acknowledge the uncertainty that comes from extrapolating from spatially limited data sets.

329 In the Dehtář fishpond, the total CH_4 fluxes increased with water depth, and this relationship was month specific.

330 The highest CH_4 fluxes at the deepest points may seem contradictory to previous studies, in which the highest

331 fluxes were typically observed in littoral areas (e.g., DelSontro et al., 2018b; Hofman et al., 2010; Natchimuthu et

332 al., 2016; Schilder et al., 2013). However, these findings are based on studying mostly large, shallow to medium-

333 deep oligotrophic lakes whose morphology, trophic state or oxygen regime sharply contrast with the hyper-

334 eutrophic Dehtář fishpond, where the upper two meters of the water column were oxygen-saturated while the

335 deepest strata were mostly anoxic, i.e., the extent and duration of bottom anoxia could be the most influential

336 factor contributing to the highest methane fluxes at the deepest point of the pond. In such hyper-eutrophic systems,

337 high nutrient loading increases autochthonous primary production (Potužák et al., 2007; Rutegwa et al., 2019) and

338 promotes oxygen consumption and anaerobic decomposition in the sediments (Baxa et al., 2020), leading to

339 enhanced CH_4 production (Bastviken et al., 2004; Grasset et al., 2018). In aquaculture ponds in Southeast China,

340 CH_4 fluxes exhibited considerable spatial variations and peaked in the relatively deep feeding zone, where the

341 large loads of sediment organic matter fueledfuelled CH_4 production (Yang et al., 2020). Furthermore, sediment

342 temperature was the strongest predictor of CH_4 fluxes in shallow ponds with anoxic hypolimnion (DelSontro et

343 al., 2016; Yang et al., 2020). It is, therefore, reasonable to assume that both temperature and oxygen concentration

344 in the sediment likely contributed to changes in observed CH_4 fluxes during the studied period in our study.

345 Although both parameters were not directly measured in the sediment, it can be deduced from their vertical profiles

346 that the probability of sediment anoxia was highest in August and lowest in September, and the sediment

347 temperature was lowest in September (see Fig. 5).

348 Our results agree with the generally accepted view that processes other than diffusive fluxes,— most likely

349 ebullition,— represent the major CH_4 pathway to the atmosphere in hyper-eutrophic ponds used for intensive fish

350 production (Kosten et al., 2020). Although freshwaters with high primary production are more likely to have high

351 CH_4 ebullition rates (DelSontro et al., 2016), the dominant role of ebullition was also found across lentic systems

352 differing in size, trophic status or geographical location (Aben et al., 2017). Ebullition accounted on average for

353 56 % of total CH_4 fluxes in northern ponds in Canada (DelSontro et al., 2016), 49 and 71 % in two different zones

354 of Lake Taihu (Xiao et al., 2017) and 48-83 % in three Swedish lakes (Natchimuthu et al., 2016; Jansen et al.,

355 2019). The highest contribution was found in the small hyper-eutrophic Priest Pot (UK), where ebullition

356 represented 96 % of the total CH_4 flux from the pond (Casper et al., 2000). Apparently, the contribution of

357 ebullition can vary among systems and will remain uncertain until measurement designs cover enough

358 spatiotemporal variability to yield representative values for the whole ecosystem.

359 In shallow water bodies, a semi-stable flux of microbubbles was suggested to account for a significant portion of

360 the total CH_4 flux (Prairie and del Giorgio, 2013). When CH_4 concentration in the water column is above a certain

361 threshold of microbubble density, these microbubbles likely aggregate, fuse, and escape to the atmosphere from

362 buoyancy (Prairie and del Giorgio, 2013). Even a small fluctuation in hydrostatic pressure (e.g., due to changes in

363 atmospheric pressure) or lake water level was shown to trigger enhanced CH_4 ebullition (Bastviken et al., 2004;

364 Casper et al., 2000; Varadharajan and Hemond, 2012). Since ebullition rates increase exponentially with

365 temperature, CH_4 fluxes tend to peak in warm summer months (van Bergen et al., 2019). In our study, 1 % lower

366 air pressure in July and August than in September, along with bottom anoxia and higher water temperature, could

367 account for the enhanced release of CH_4 bubbles from the sediment (31.7 mmol $m^{-2}d^{-1}$, >90 % of total CH_4 fluxes;

368 Suppl. Fig. 2). In September, when we observed the lowest water temperatures from the studied period and the

369 oxygen profile was rather uniform, ebullition accounted for 81 % (11 mmol $m^{-2}d^{-1}$) of the total CH_4 fluxes. The

370 spatially pooled data of the total CH_4 fluxes measured in the Dehtář fishpond varied from 11.8 to 34.5 mmol m^{-2}

371 d^{-1}, which is comparable with similar systems elsewhere (e.g., Bastviken et al., 2010; van Bergen et al., 2019;

372 Baron et al., 2022). To sum up, both diffusive fluxes and ebullition must be addressed to understand the magnitude

373 of total aquatic CH_4 fluxes and how their relative contributions vary across and within aquatic systems (Kosten et

374 al., 2020). Moreover, with an improved determination of CH_4 hot-spots and its causes, the management of ponds

375 could be changed accordingly and so the overall emissions reduced for example by decreasing P-availability and

376 dredging (Nijman et al., 2022).

377 **4.2 Effect of wind event on ecosystem spatial structure**

378 Sudden changes in ecosystem spatial structure in response to meteorological forcing have rarely been documented

379 (Loken et al., 2019) since they are hard to predict. Research into them using traditional methods requires intensive

380 effort or expensive instrumentation (Ortiz and Wilkinson, 2021), and it remains a matter of luck to obtain a relevant

381 dataset. In the July sampling campaign, we observed a strong impact of the wind on environmental heterogeneity

382 in the fishpond, which was apparent at a sub-daily time scale. Due to the methodological constraints, i.e., lack of

383 initial measurement, we can only speculate about the effect of wind on the total CH_4 fluxes. The northwest wind

384 during the day advected warmed surface water with cyanobacterial bloom from the north basin to the south. In the

385 evening, it resulted in bloom accumulation on the upward side and a north-south gradient of more than 4 °C and

386 4 2420 mg L^{-1} oxygen. After the winds fell off, the observed gradients declined during cooling at night. We assume

387 that the wind blowing across the pond surface drove buoyant cyanobacteria and surface water downwind and

388 caused an upwelling of deeper, colder, and hypoxic water on the upwind side. This wind-related circulation pattern

has been described as a "conveyer belt" in classical textbooks (Reynolds et al., 2006), held responsible for a disruption of the thermal structure of the water column and the non-uniform spatial distribution of pH, oxygen, CO_2 or CH_4 and also plankton assemblages (e.g., Loken et al., 2019; Natchimuthu et al., 2016; Rinke et al., 2009; Ortiz and Wilkinson, 2021).

Similar to our study, mild winds (~4 m s^{-1}) were strong enough to redistribute heat and induce lake-wide circulations driving upwelling and downwelling in 24 m deep Lake Pleasant (Czikowsky et al., 2018). As the wind blows harder and lasts longer, the effects on ecosystem functioning may target higher trophic levels and become more complex (Rinke et al., 2009). In Lake Constance, a three-day storm event with wind velocities of ~10 m s^{-1} resulted in a lake-wide displacement of water masses and the formation of the 6–15 °C horizontal surface water gradient, which in turn changed the spatial distribution of phytoplankton, zooplankton and juvenile fish (Rinke et al., 2009). After several stormy days (wind velocities of 12–15 m s^{-1}), Čech et al. (2011) observed negative effects of wind-driven changes in water temperature and wave action on perch (*Perca fluviatilis*) spawning in the Lake Milada. Although wind events affect shallow and deep lakes differently, there is growing evidence that they can have far-reaching consequences on the functioning of aquatic ecosystems by disrupting energy flows, nutrient fluxes, productivity and reproduction, and consequently altering community composition and trophic interactions in the short and long term (Stockwell et al., 2020). As the frequency, intensity, spatial extent and duration of these extreme meteorological events are projected to increase due to ongoing climate change (Comou and Rahmstorf, 2012), there is an urgent need to better understand the mechanisms underlying their impacts on the maintenance of the ecosystem services.

4.3 Summer changes in the oxygen regime

Our data demonstrate that shallow, hyper-eutrophic ponds have disrupted oxygen regimes (Baxa et al., 2021) with anoxic hypolimnion and may experience severe whole-water column hypoxia critical for aquatic biota (Miranda et al., 2001). The hypoxic periods may result, for example, from sudden weather change (Jeppesen et al., 1990) and last several days, during which physical processes and phytoplankton photosynthesis cannot compensate for intense community respiration (Baxa et al., 2021). This became obvious in August when severe oxygen depletion was measured at the surface across the whole pond, mostly far below a critical level of 4.5 mg L^{-1}, when adverse effects came into play (Banerjee et al., 2019). However, oxygen surface concentrations in shallow parts of the pond were substantially higher regardless of the time of day, which contrasts with findings of Miranda et al. (2001), who emphasised shallow waters as the most sensitive parts of lakes, where hypoxic events can occur due to the respiration of sediment biota. The observed spatial gradients of oxygen may create temporal refugia which allow

419 fish to survive harsh conditions that occur in the deepest part of the pond. To minimise economic losses and

420 negative impacts on the ecosystem, future research should identify the interplay between meteorological forcing,

421 trophic status and anthropogenic pressures (e.g., management practices) that affect oxygen fluctuations at various

422 time scales.

423 **4.4 Study limitations**

424 Like in other research, there are some limitations in the current study. Since our measurement had only a limited

425 temporal resolution (three samplings during the summer season), it is not appropriate to extrapolate CH_4 emissions

426 for annual values. Noticeably, future research must increase the frequency of the sampling and include also

427 innovative techniques to measure CH_4 fluxes at multiple fishponds, with different management regime. In our

428 study, the 12-h deployment time of the floating chambers could have led to extensive gas accumulation, which in

429 turn might have resulted in an underestimation of the total CH_4 fluxes due to the dissolution of the CH_4 from the

430 chamber into the water once the equilibrium concentration in the chamber is overcome (Bastviken et al., 2010).

431 However, CH_4 concentrations in water corresponded to a supersaturation of several orders of magnitude, so the

432 introduced bias appears to be of minor importance. In any case, our daily spatially pooled total CH_4 fluxes (11.8–

433 34.5 mmol m^{-2} d^{-1}) represent a rather conservative estimate for the global methane budget. In our study, we also

434 did not address the important processes that could shed light on the lake CH_4 budget, such as CH_4 oxidation rates

435 (Bastviken et al., 2008) or biological interaction (e.g., protistan grazing on CH_4 oxidising bacteria) in aquatic food

436 webs (Sanseverino et al., 2012) that can affect the overall CH_4 fluxes. We also lack information about spatial

437 differences in sediment microbiota and organic carbon content and compositions, which were found to affect CH_4

438 production rates (Berberich et al., 2020; Emerson et al., 2021). Despite the limitation mentioned above, our results

439 show that complementary spatial surveys help contextualise the fixed station dynamics and provide additional,

440 management-relevant information about the fishpond.

441 For improved monitoring strategies, however, a continuous measurement approach like eddy covariance would be

442 generally more efficient than traditional sampling at regular intervals. Eddy covariance accounts for temporal

443 variability and provides high temporal resolution data by continuously measuring wind speed, gas concentration,

444 and vertical turbulent fluxes to estimate methane emissions (Erkkilä et al., 2018). More importantly, it also offers

445 spatially integrated measurements, averaging emissions over a larger area and therefore accounts for pond spatial

446 heterogeneity. However, it's worth noting that the choice of monitoring approach depends on various factors,

447 including the specific objectives, available resources, and the characteristics of the emission sources. To accurately

448 capture both short-term variability and lake spatial heterogeneity of methane ebullition and diffusion fluxes, the

most efficient approach was found to be a combination of continuous measurements with traditional methods including floating chambers, anchored funnels and boundary model calculations (Schubert et al., 2012; Podgrajsek et al., 2014; Erkkilä et al., 2018). This integrated approach would provide a comprehensive understanding of methane emissions, enabling better estimation and more effective mitigation efforts.

5 Conclusions

Many fishponds are hundreds of years old (Potužák et al., 2007), and as such, they are an integral part of our cultural heritage. Nowadays, ponds face a variety of conflicting interests often leading to a focus on maximising fish production that comes at the expense of other ecological services. Intensification of fish production has brought a transition from the traditional management based on natural processes to practices involving supplementary feeding, fertilisation, and overstocking (Pechar, 2000). These changes coupled with the impacts of climate change has resulted to frequent anoxic events and cyanobacterial blooms that reduce biodiversity and limit recreational activities increasingly valued by the public. Our study not only illustrates common water quality problems in fishponds but also provides compelling evidence that methane emissions in these degraded ecosystems further exacerbates negative climate feedbacks and should be considered in discussions to advance the development of sustainable management.

Deciphering the mechanisms that drive spatial and temporal heterogeneity in aquatic ecosystem structure and function not only expands our understanding of pond ecology but also provides insights to improve the management of these ecosystems and the services they provide. Our results suggest that spatial heterogeneity needs to be considered when designing experiments and monitoring programs. Without the spatially resolved sampling, we introduce bias into our datasets, hampering our limnological understanding of the ecosystem's functioning and impeding our ability to accurately estimate rates such as methane emissions on a global scale (DelSontro et al., 2018a). In agreement with Kosten et al. (2020), we demonstrated that neglecting ebullition leads to a considerable underestimating of the total CH_4 fluxes. Since there are thousands of these intensively managed fishponds, we argue for changing the management practices toward sustainable use of natural resources to mitigate the overall emissions of greenhouse gases from these ecosystems. Future studies are needed to characterise CH_4 fluxes over a greater number and diversity of aquaculture ponds and examine the mechanisms controlling CH_4 emissions in aquatic ecosystems.

Acknowledgements

The study was supported by the Czech Science Foundation (Research Projects No. 17-09310S, 19-23261S and P504/19-16554S). We thank Martin Rulík for providing us gas chambers. We especially thank to Miloslav Šimek and Linda Jíšová for enabling gas analyses. We are grateful Anna Sieczko for consultation on the calculation of CH_4 fluxes. English correction was made by Anton Baer.

Data availability

Dataset associated with the manuscript can be found in the GitHub Repositories under https://zenodo.org/badge/latestdoi/587640213.

Author contributions

All authors contributed to the study conception and design. PZ planned the campaign; PZ, AM and JN performed the sampling and analyzed the data; AM performed the gas-measurements; VK performed statistical analyses and modelling; PZ and AM wrote the manuscript. All authors read and approved the final manuscript.

References

Aben, R.C.H., Barros, N., van Donk, E., Frenken, T., Hilt, S., Kazanjian, G., Lamers, L.P.M., Peeters, E.T.H.M., Roelofs, J.G. M, de Senerpont Domis, L.N., Stephan, S., Velthuis, M., Van de Waal, D.B., Wik, M., Thornton, B.F., Wilkinson, J., DelSontro, T., and Kosten, S.: Cross continental increase in methane ebullition under climate change. Nat. Commun., 8, 1682, https://doi.org/10.1038/s41467-017-01535-y, 2017.

Banerjee, A., Chakrabarty, M., Rakshit, N., Bhowmick, A.R., and Ray, S.: Environmental factors as indicators of dissolved oxygen concentration and zooplankton abundance: deep learning versus traditional regression approach. Ecol. Indic., 100, 99-117, https://doi.org/10.1016/j.ecolind.2018.09.051, 2019.

Baron, A.A.P., Dyck, L.T., Amjad, H., Bragg, J., Kroft, E., Newson, J., Oleson, K., Casson, N.J., North, R.L., Venkiteswaran, J.J., and Whitfield, C.J.: Differences in ebullitive methane release from small, shallow ponds present challenges for scaling. Sci. Total Environ., 802, 149685, https://doi.org/10.1016/j.scitotenv.2021.149685, 2022.

Bartosiewicz, M., Maranger, R., Przytulska, A., and Laurion, I.: Effects of phytoplankton blooms on fluxes and emissions of greenhouse gases in a eutrophic lake. Water Res., 196, 116985, https://doi.org/10.1016/j.watres.2021.116985, 2021.

Bastviken, D., Cole, J., Pace M., and Tranvik, L.: Methane emissions from lakes: Dependence of lake characteristics, two regional assessments, and a global estimate. Global Biogeochem. Cycles, 18, GB4009, https://doi.org/10.1029/2004GB002238, 2004.

506 Bastviken, D., Cole, J.J., Pace, M.L., and Van de Bogert, M.C.: Fates of methane from different lake habitats:
507 connecting whole-lake budgets and CH_4 emissions. J. Geophys. Res. Biogeosci., 113, G02024,
508 https://doi.org/10.1029/2007JG000608, 2008.

509 Bastviken, D., Santoro, A.L., Marotta, H., Pinho, L.Q., Calheiros, D.F., Crill, P., and Enrich-Prast, A.: Methane
510 Emissions from Pantanal, South America, during the Low Water Season: Toward More Comprehensive Sampling.
511 Environ. Sci. Tech., 44, 5450-5455, https:///doi.org/10.1021/es1005048, 2010.

512 Bates, D., Maechler, M., Bolker, B., and Walker, S.: Fitting Linear Mixed-Effects Models Using lme4. J. Stat.
513 Soft., 67, 1-48, https://doi.org/10.18637/jss.v067.i01, 2015.

514 Baxa, M., Musil, M., Kummel, M., Hazlík, O., Tesařová, B., and Pechar, L.: Dissolved oxygen deficits in a shallow
515 eutrophic aquatic ecosystem (fishpond) – Sediment oxygen demand and water column respiration alternately drive
516 the oxygen regime. Sci. Total Environ., 766, 142647, https://doi.org/10.1016/j.scitotenv.2020.142647, 2021.

517 Berberich, M.E., Beaulieu, J.J., Hamilton, T.L., Waldo, S., and Buffam, I.: Spatial variability of sediment methane
518 production and methanogen communities within a eutrophic reservoir: Importance of organic matter source and
519 quantity. Limnol. Oceanogr., 65, 1336-1358, https://doi.org/10.1002/lno.11392, 2020.

520 Bižić, M., Klintzsch, T., Ionescu, D., Hindiyeh, M.Y., Günthel, M., Muro-Pastor, A.M., Eckert, W., Urich, T.,
521 Keppler, F., and Grossart, H.P.: Aquatic and terrestrial cyanobacteria produce methane. Sci. Adv., 6, 1-10,
522 https://doi.org/10.1126/sciadv.aax5343, 2020.

523 Bussmann, I., Matoušů, A., Osudar, R., and Mau, S.: Assessment of the radio ^{3}H-CH_4 tracer technique to measure
524 aerobic methane oxidation in the water column. Limnol. Oceanogr.- Meth., 13, 312-327,
525 https://doi.org/10.1002/lom3.10027, 2015.

526 Casper, P., Maberly, S.C., Hall, G.H., and Finlay, B.J.: Fluxes of methane and carbon dioxide from a small
527 productive lake to the atmosphere. Biogeochemistry, 49, 1-19, https://doi.org/10.1023/A:1006269900174, 2000.

528 Čech, M., Peterka, J., Říha, M., Muška, M., Hejzlar, J., and Kubečka, J.: Location and timing of the deposition of
529 eggs strands by perch (*Perca fluviatilis* L.): the roles of lake hydrology, spawning substrate and female size.
530 Knowl. Manag. Aquat. Ecosyst., 403, 1-12, https://doi.org/10.1051/kmae/2011070, 2011.

531 Céréghino, R., Biggs, J., Oertli, B., and Declerck, S.: The ecology of European ponds: defining the characteristics
532 of a neglected freshwater habitat. Hydrobiologia, 597, 1-6, https://doi.org/10.1007/s10750-007-9225-8, 2008.

533 Coumou, D. and Rahmstorf, S.: A decade of weather extreme. Nat. Clim. Change, 2, 491-96,
534 https://doi.org/10.1038/nclimate1452, 2012.

535 Crusius, J. an Wanninkhof, R.: Gas transfer velocities measured at low wind speed over a lake. Limnol. Oceanogr.,
536 48, 1010-1017, https://doi.org/10.4319/lo.2003.48.3.1010, 2003.

537 Czikowsky, M.J., MacIntyre, S., Tedford, E.W., Vidal, J., and Miller, S.D.: Effects of wind and buoyancy on
538 carbon dioxide distribution and air-water flux of a stratified temperate lake. J. Geophys. Res. Biogeosci., 123,
539 2305-2322, https://doi.org/10.1029/2017JG004209, 2018.

540 De Meester, L., Declerck, S., Stoks, R., Louette, G., Van de Meutter, F., De Bie, T., Michels, E., and Brendonck,
541 L.: Ponds and pools as model systems in conservation biology, ecology and evolutionary biology. Aquat. Cons.,
542 15, 715-725, https://doi.org/10.1002/aqc.748, 2005.

543 DelSontro, T., Boutet, L., St-Pierre, A., del Giorgio, P.A., and Prairie, Y.T.: Methane ebullition and diffusion from
544 northern ponds and lakes regulated by the interaction between temperature and system productivity. Limnol.
545 Oceanogr., 61, 62-77, https://doi.org/10.1002/lno.10335, 2016.

546 DelSontro, T., Beaulieu, J.J., and Downing, J.J.: Greenhouse gas emissions from lakes and impoundments:
547 upscaling in the face of global change. Limnol. Oceanogr. Lett., 3, 64-75, https://doi.org/10.1002/lol2.10073,
548 2018a.

549 DelSontro, T., del Giorgio, P.A., and Prairie, Y.T.: No Longer a Paradox: The Interaction Between Physical
550 Transport and Biological Processes Explains the Spatial Distribution of Surface Water Methane Within and Across
551 Lakes. Ecosystems, 21, 1073-1087, 10.1007/s10021-017-0205-1, 2018b.

552 Emerson, J.B., Varner, R.K., Wik, M., Parks, D.H., Neumann, R.B., Johnson, J.E., Singleton, C. M., Woodcroft,
553 B.J., Tollerson II, R., Owusu-Dommey, A., Binder, M., Freitas, N. L., Crill, P.M., Saleska, S.R., Tyson, G.W., and
554 Rich, V.I.: Diverse sediment microbiota shape methane emission temperature sensitivity in Arctic lakes. Nat.
555 Commun., 12, 5815, https://doi.org/10.1038/s41467-021-25983-9, 2021.

556 Erkkilä, K.-M., Ojala, A., Bastviken, D., Biermann, T., Heiskanen, J. J., Lindroth, A., Peltola, O., Rantakari, M.,
557 Vesala, T., and Mammarella, I.: Methane and carbon dioxide fluxes over a lake: comparison between eddy
558 covariance, floating chambers and boundary layer method, Biogeosciences, 15, 429–445,
559 https://doi.org/10.5194/bg-15-429-2018, 2018.

560 Grasset, Ch., Mendonça, R,., Saucedo, G.V., Bastviken, D., Roland, F., and Sobek, S.: Large but variable methane
561 production in anoxic freshwater sediment upon addition of allochthonous and autochthonous organic matter.
562 Limnol. Oceanogr., 63, 1488-1501, https://doi.org/10.1002/lno.10786, 2018.

563 Halekoh, H. and Hojsgaard, S.: A Kenward-Roger Approximation and Parametric Bootstrap Methods for Tests in
564 Linear Mixed Models - The R Package pbkrtest. J. Stat. Soft., 59, 1-30, https://doi.org/10.18637/jss.v059.i09 2014.

565 Hofmann, H., Federwisch, L., and Peeters, F.: Wave-induced release of methane: littoral zones as a source of
566 methane in lakes. Limnol. Oceanogr., 55, 1990-2000, https://doi.org/10.4319/lo.2010.55.5.1990, 2010.

567 Hofmann, H.: Spatiotemporal distribution patterns of dissolved methane in lakes: How accurate are the current
568 estimations of the diffusive flux path? Geophys. Res. Lett., 40, 2779-2784, https://doi.org/10.1002/grl.50453,
569 2013.

570 Hu, Z., Wu, S., Ji, Ch., Zou, J., Zhou, Q., and Liu, S.: A comparison of methane emissions following rice paddies
571 conversion to crab-fish farming wetlands in southeast China. Environ. Sci. Pollut. Res., 23, 1505-1515,
572 https://doi.org/10.1007/s11356-015-5383-9, 2016.

573 Jansen, J., Thornton, B.F., Jammet, M.M., Wik, M., Cortés, A., Friborg, T., MacIntyre, S., and Crill, P.M.:
574 Climate-sensitive controls on large spring emissions of CH_4 and CO_2 from northern lakes. J. Geophys. Res.,
575 Biogeosciences, 124, 2379-2399, https://doi.org/10.1029/2019JG005094, 2019.

576 Jähne, B., Münnich, K. O., Bösinger, R., Dutzi, A., Huber, W., and Libner, P.: On the parameters influencing air-
577 water gas exchange, J. Geophys. Res., 92, C2, 1937-1949, doi:10.1029/JC092iC02p01937, 1987.

578 Jeppesen, E., Søndergaard, M., Sortkjaer, O., Mortensen, E., and Kristensen, P.: Interactions between
579 phytoplankton zooplankton and fish in a shallow hypertrophic Lake a study of phytoplankton collapses in Lake
580 Sobygaard, Denmark. Hydrobiologia, 1991, 149-164, https://doi.org/10.1007/BF00026049, 1990.

581 Kolar, V., Vlašánek, P., and Boukal, D.S.: The influence of successional stage on local odonate communities in
582 man-made standing waters. Ecol. Eng., 173, 106440, https://doi.org/10.1016/j.ecoleng.2021.106440, 2021.

583 Kopáček, J. and Hejzlar, J.: Semi-micro determination of total phosphorus in fresh waters with perchloric acid
584 digestion. Int. J. Environ. Anal. Chem., 53, 173-183, https://doi.org/10.1080/03067319308045987, 1993.

Kopáček, J. and Procházková, L.: Semi-Micro Determination of Ammonia in Water by the Rubazoic Acid Method. Int. J. Environ. Anal. Chem., 53, 243-248, https://doi.org/10.1080/03067319308045993, 1993.

Kosten, S., Almeida, R.M., Barbosa, I., Mendonça, R., Muzitano, I.S., Oliveira-Junior, E.S., Vroom, R.J.E., Wang, H.J., and Barros, N.: Better assessments of greenhouse gas emissions from global fish ponds needed to adequately evaluate aquaculture footprint. Sci. Total Environ., 748, 141247, https://doi.org/10.1016/j.scitotenv.2020.141247, 2020.

Laas, A., Noges, P., Koiv, T., and Noges, T.: High-frequency metabolism study in a large and shallow temperate lake reveals seasonal switching between net autotrophy and net heterotrophy. Hydrobiologia, 694, 57-74, https://doi.org/10.1007/s10750-012-1131-z, 2012.

Loken, L.C., Crawford, J.T., Schramm, P.J., Stadler, P., Desai, A.R., and Stanley, E.H.: Large spatial and temporal variability of carbon dioxide and methane in a eutrophic lake. J. Geophys. Res. Biogeosci., 124, 2248-2266 https://doi.org/10.1029/2019JG005186, 2019.

Lüdecke, D.: "ggeffects: Tidy Data Frames of Marginal Effects from Regression Models." J. Open Source Soft., 3, 772, https://doi: 10.21105/joss.00772, 2018.

Lüdecke, D., Makowski, D., and Waggoner, P.: performance: Assessment of Regression Models Performance. R package version 0.4.4. https://CRAN.R-project.org/package=performance, 2020.

Ma, Y., Sun, L., Liu, C., Yang, X., Zhou, W., Yang, B., Schwenke, G., and Liu, D.L.: A comparison of methane and nitrous oxide emissions from inland mixed-fish and crab aquaculture ponds. Sci. Total Environ., 637-638, 517-523, https://doi.org/10.1016/j.scitotenv.2018.05.040, 2018

McAuliffe, C.: Gas Chromatographic determination of solutes by multiple phase equilibrium. Chem. Technol., 1, 46-51, 1971.

Miranda, L.E., Hargreaves, J.A., and Raborn, S.W.: Predicting and managing risk of unsuitable dissolved oxygen in a eutrophic lake. Hydrobiologia, 457, 177-185, https://doi.org/10.1023/A:1012283603339, 2001.

Murphy, J. and Riley, J.P.: A modified single-solution method for the determination of phosphate in natural waters. Anal. Chim. Acta, 27, 31-36, https://doi.org/10.1016/S0003-2670(00)88444-5, 1962.

Natchimuthu, S., Sundgren, I., Gålfalk, M., Klemedtsson, L., Crill, P., Danielsson, Å., and Bastviken, D.: Spatio-temporal variability of lake CH_4 fluxes and its influence on annual whole lake emission estimates. Limnol. Oceanogr., 61, 13-26, https://doi.org/10.1002/lno.10222, 2016.

Nijman, T.P.A., Lemmens, M., Lurling, M., Kosten, S., Welte, C., and Veraart, A.J.: Phosphorus control and dredging decrease methane emissions from shallow lakes. Sci. Total Environ., 847, 15758, https://doi.org/10.1016/j.scitotenv.2022.157584, 2022.

Ortiz, D.A. and Wilkinson, G.M.: Capturing the spatial variability of algal bloom development in a shallow temperate lake. Freshwater Biol., 66, 2064-2075, https://doi.org/10.1111/fwb.13814, 2021.

Pechar, L.: Impacts of long-term changes in fishery management on the trophic level and water quality in Czech fishponds. Fisheries Manag. Ecol., 7, 23-32, 10.1046/j.1365-2400.2000.00193.x, 2000.

Pokorný, J. and Hauser, V.: The restoration of fish ponds in agricultural landscapes. Ecol. Eng., 18, 555-574, https://doi.org/10.1016/S0925-8574(02)00020-4, 2002.

Podgrajsek, E., Sahlée, E., Bastviken, D., Holst, J., Lindroth, A., Tranvik, L., and Rutgersson, A.: Comparison of floating chamber and eddy covariance measurements of lake greenhouse gas fluxes, Biogeosciences, 11, 4225–4233, https://doi.org/10.5194/bg-11-4225-2014, 2014.

Potužák, J., Hůda, J., and Pechar, L.: Changes in fish production effectivity in eutrophic fishponds – impact of zooplankton structure. Aquacult. Int., 15, 201-210, https://doi.org/10.1007/s10499-007-9085-2, 2007.

Potužák, J., Duras, J., and Drozd, B.: Mass balance of fishponds: are they sources or sinks of phosphorus? Aquacult. Int., 24, 1725-1745, https://doi.org/10.1007/s10499-016-0071-4, 2016.

Prairie, Y.T. and del Giorgio, P.A.: A new pathway of freshwater methane emissions and the putative importance of microbubbles. Inland Waters, 3, 311-320, https://doi.org/10.5268/IW-3.3.542, 2013.

Procházková, L.: Bestimmung der Nitrate im Wasser. Zeitschrit für Analytische Chemie, 167, 254-260, 1959.

Rasilo, T., Prairie, Y.T., and del Giorgio, P.A.: Large-scale patterns in summer diffusive CH_4 fluxes across boreal lakes, and contribution to diffusive C emissions. Glob. Change Biol., 21, 1124-1139, https://doi.org/10.1111/gcb.12741, 2015.

R Core Team: A language and environment for statistical computing. R Foundation for Statistical Computing. Vienna, Austria https://www.R-project.org/, 2018.

Reynolds, C.S.: Ecology of phytoplankton, Cambridge University Press, Cambridge, https://doi.org/10.1017/CBO9780511542145, 2006.

Rinke, K., Huber, A.M.R., Kempke, S., Eder, M., Wolf, T., Probst, W.N., and Rothhaupt, K.: Lake-wide distributions of temperature, phytoplankton, zooplankton, and fish in the pelagic zone of a large lake. Limnol. Oceanogr., 54, 1306-1322, https://doi.org/10.4319/lo.2009.54.4.1306, 2009.

Rutegwa, M., Potužák, J., Hejzlar, J., and Drozd, B.: Carbon metabolism and nutrient balance in a hypereutrophic semi-intensive fishpond. Knowl.Manag. Aquat. Ecosyst., 49, https://doi.org/10.1051/kmae/2019043, 2019.

Sanseverino, A.M., Bastviken, D., Sundh, I., Pickova, J., and Enrich-Prast, A.: Methane carbon supports aquatic food webs to the fish level. PLoS One7, e42723, https://doi.org/10.1371/journal.pone.0042723, 2012.

Scheffer, M.: Ecology of shallow lakes. Population and Community Biology Series. Springer, 357 p., https://doi.org/10.1007/978-1-4020-3154-0, 2004.

Schilder, J., Bastviken, D., van Hardenbroek, M., Kankaala, P., Rinta, P., Stötter, T., and Heiri, O.: Spatial heterogeneity and lake morphology affect diffusive greenhouse gas emission estimates of lakes. Geophys. Res. Lett., 40, 5752-5756, https://doi.org/10.1002/2013GL057669, 2013.

Schmiedeskamp, M., Praetzel, L.S.E., Bastviken, D., and Knorr, K.H.: Whole-lake methane emissions from two temperate shallow lakes with fluctuating water levels: Relevance of spatiotemporal patterns. Limnol. Oceanogr., 66, 2455-2469, https://doi.org/10.1002/lno.11764, 2021.

Schubert, C.J., Diem, T., Eugster W.: Methane emissions from a small wind shielded lake determined by eddy covariance, flux chambers, anchored funnels, and boundary model calculations: a comparison. Environ. Sci. Technol., 46, 4515-4522, https://doi.org/10.1021/es203465x, 2012

Stanley, E.H., Collins, S.M., Lottig, N.R., Oliver, S.K., Webster, K.E., Cheruvelil, K.S., and Soranno, P.A.: Biases in lake water quality sampling and implications for macroscale research. Limnol. Oceanogr., 64, 1572-1585, https://doi.org/10.1002/lno.11136, 2019.

Stockwell, J.D., Doubek, J.P., Adrian, R., Anneville, O., Carey, C.C., Carvalho, L., Domis, L.N.D.S., Dur, G., Frassl, M.A., Grossart, H.-P., Ibelings, B.W., Lajeunesse, M.J., Lewandowska, A.M., Llames, M.E., Matsuzaki, S.-I.S., Nodine, E.R., Nõges, P., Patil, V.P., Pomati, F., Rinke, K., Rudstam, L.G., Rusak, J.A., Salmaso, N., Seltmann, C.T., Straile, D., Thackeray, S.J., Thiery, W., Urrutia-Cordero, P., Venail, P., Verburg, P., Woolway, R.I., Zohary, T., Andersen, M.R., Bhattacharya, R., Hejzlar, J., Janatian, N., Kpodonu, A.T.N.K., Williamson,

T.J., and Wilson, H.L.: Storm impacts on phytoplankton community dynamics in lakes. Glob. Change Biol., 26, 2756-2784, https://doi.org/10.1111/gcb.15033, 2020.

van Bergen, T.J.H.M., Barros, N., Mendonça, R., Aben, R.C.H., Althuizen, I.H.J., Huszar, V.,Lamers, L.P.M., Lürling, M., Roland, F., Kosten, S.: Seasonal and diel variation in greenhouse gas emissions from an urban pond and its major drivers. Limnol. Oceanog., 64, 2129-2139, https://doi.org/10.1002/lno.11173, 2019.

Varadharajan, Ch. and Hemond, H.F.: Time-series analysis of high-resolution ebullition fluxes from a stratified, freshwater lake. J. Geophys. Res., 117, G02004, https://doi.org/10.1029/2011JG001866, 2012.

Wanninkhof, R.: Relationship between wind speed and gas exchange over the ocean revisited. Limnol. Oceanogr. Methods, 12, 351-362, https://doi.org/10.4319/lom.2014.12.351, 2014.

Wiesenburg, D.A. and Guinasso N.L.: Equilibrium solubilities of methane, carbon monoxide, and hydrogen in water and sea water. J. Chem. Eng. Data, 24, 356-360, https://doi.org/10.1021/je60083a006, 1979.

Wik, M., Varner, R.K., Anthony, K.W., MacIntyre, S., and Bastviken, D.: Climate-sensitive northern lakes and ponds are critical components of methane release. Nat. Geosci., 9, 99-105, https://doi.org/10.1038/ngeo2578, 2016.

Xiao, Q., Zhang, M., Hu, Z., Gao, Y., Hu, Ch., Liu, Ch., Liu, S., Zhang, Z., Zhao, J., Xiao, W., and Lee, X.: Spatial variations of methane emission in a large shallow eutrophic lake in subtropical climate. J. Geophys. Res. Biogeosci., 122, https://doi.org/10.1002/2017JG003805, 2017.

Yamamoto, S., Alcauskas, J.B., and Crozier, T.E. Solubility of methane in distilled water and seawater. J. Chem. Eng. Data, 21, 78-80, https://doi.org/10.1021/je60068a029, 1976.

Yan, X., Xu, X., Ji, M., Zhang, Z., Wang, M., Wu, S., Wang, G., Zhang, Ch., and Liu, H.: Cyanobacteria blooms: A neglected facilitator of CH_4 production in eutrophic lakes. Sci. Total Environ., 651, 466-474, https://doi.org/10.1016/j.scitotenv.2018.09.197, 2019.

Yang, P., Zhang, Y., Yang, H., Zhang, Y., Xu, J., Tan, L., Tong, C., and Lai, D.Y.: Large fine-scale spatiotemporal variations of CH_4 diffusive fluxes from shrimp aquaculture ponds affected by organic matter supply and aeration in Southeast China. J. Geophys. Res. Biogeosci., 124, 1290-1307, https://doi.org/10.1029/2019JG005025, 2019.

Yang, P., Zhang, Y., Yang, H., Guo, Q., Lai, D.Y.F., Zhao, G., Li, L., and Tong, C.: Ebullition was a major pathway of methane emissions from the aquaculture ponds in Southeast China. Water Res., 184, 116176, https://doi.org/10.1016/j.watres.2020.116176, 2020.

Yuan, J., Xiang, J., Liu, D.Y., Kang, H., He, T.H., Kim, S., Lin, Y.X., Freeman, C., and Ding, W.X.: Rapid growth in greenhouse gas emissions from the adoption of industrial-scale aquaculture. Nat. Clim. Chang., 9, 318-322, https://doi.org/10.1038/s41558-019-0425-9, 2019.

Yuan, J., Liu, D., Xiang, J., He, T., Kang, H., and Ding, W.: Methane and nitrous oxide have separated production zones and distinct emission pathways in freshwater aquaculture ponds. Water Research, 190, 116739, https://doi.org/10.1016/j.watres.2020.116739, 2021.

Zar, J.H.: Biostatistical analysis. Prentice Hall, Inc., Englewood Cliffs, New York, 663 p., 1984.

Zhang, L., Liao, Q., Gao, R., Luo, R., Liu, Ch., Zhong, J., and Wang, Z.: Spatial variations in diffusive methane fluxes and the role of eutrophication in a subtropical shallow lake. Sci. Total Environ., 759, 143495, https://doi.org/10.1016/j.scitotenv.2020.143495, 2021.

703   Zhao, J., Zhang, M., Xiao, W., Jia, L., Zhang, X., Wang, J., Zhang, Z., Xie, Y., Yini Pu, Liu, S., Feng, Z., Lee X.:

704   Large methane emission from freshwater aquaculture ponds revealed by long-term eddy covariance observation.

705   Agric. For. Meteorol., 308-309, 108600, https://doi.org/10.1016/j.agrformet.2021.108600, 2021.

706   Zhou, Y.Q., Zhou, L., Zhang, Y.L., de Souza, J.G., Podgorski, D.C., Spencer, R.G.M., Jeppesen, E., and Davidson,

707   T.A.: Autochthonous dissolved organic matter potentially fuels methane ebullition from experimental lakes. Water

708   Res., 166, 115048, https://doi.org/10.1016/j.watres.2019.115048, 2019.

709   Zuur, A.F., Ieno, E.N., Walker, N.J., Saveliev, A.A., and Smith, G.M.: Mixed effects models and extensions in

710   ecology with R. Springer, New York, USA, 574 p, https://doi.org/10.1007/978-0-387-87458-6, 2009.